Energy 61 (2013) 440–446

Contents lists available at ScienceDirect

Energy

journal homepage: www.elsevier.com/locate/energy

Kinetic studies on carbon dioxide capture using lignocellulosic based activated carbon

Nor Adilla Rashidi [a], Suzana Yusup [a, *], Bassim H. Hameed [b]

[a] Chemical Engineering Department, Universiti Teknologi PETRONAS, Bandar Seri Iskandar, 31750 Tronoh, Perak, Malaysia
[b] School of Chemical Engineering, Universiti of Science Malaysia, Engineering Campus, Seri Ampangan, 14300 Nibong Tebal, Pulau Pinang, Malaysia

ARTICLE INFO

Article history:
Received 28 February 2013
Received in revised form
17 July 2013
Accepted 25 August 2013
Available online 21 September 2013

Keywords:
Activated carbon
Adsorption
CO_2 capture

ABSTRACT

CO_2 (Carbon dioxide) emissions are one of the greenhouse gases that cause global warming. The power generation industry is one of the main emitters of CO_2, and the emissions are expected to increase in the coming years as there seems to be no abatement in the consumption of fossil fuels for the production of electricity. Thus, there is a need for CO_2 adsorption technologies to mitigate the emissions. However, there are several disadvantages associated with the current adsorption technologies. One of the issues is corrosion and the need for specialized equipment. Therefore, alternative and more sustainable materials are sought after to improve the viability of the adsorption technology. In this study, several types of agricultural wastes were used as activated carbon precursors for CO_2 adsorption process in a TGA (thermogravimetric analyser). The adsorption was also modelled through a pseudo-first order and second order model, Elovich's kinetic model, and an intra-particle diffusion model. From the correlation coefficient, it was found that pseudo-second order model was well-fitted with the kinetic data. In addition, activation energy below than 42 kJ/mol confirmed that the physisorption process occurred.

1. Introduction

Over the past decades, global warming has become a serious issue, and has prompted efforts to reduce greenhouse gas emissions, especially CO_2 (carbon dioxide) [1]. Combustion of coal in power plants is one of the main sources of CO_2 emissions, and coal remains the preferred fuel due to its abundance and cheaper cost, which is the case in Malaysia [2]. In Malaysia, there is reportedly 1.724 billion tonnes of coal reserves located mostly in West Malaysia [3]. With a secured supply of coal, the consumption of coal is expected to increase for the next decade (as shown in Table 1). Thus, the corresponding CO_2 emissions are expected to increase to approximately 285 million tonnes by 2020 [1]. To mitigate CO_2 emissions, various technologies have been proposed, such as chemical absorption (amine scrubbing), solid adsorption, cryogenic process and membrane separation process [5]. Among these technologies, chemical absorption with aqueous amine-based solvent such as MEA (monoethanolamine) has been applied in industries [5]. However, there are several disadvantages associated with this technology, which include problems of corrosion, the need for special materials for equipment construction, a high energy penalty for regeneration process, and the degradation of amine under the oxidizing environment of flue gas from the power plants [6]. Thus, an alternative material is required to overcome the limitations of this existing technology. Solid adsorption using the activated carbon is one of the most prominent alternatives as it is easy to handle, widely available, and is good in terms of moisture removal [7]. Though research on activated carbon production is widely performed, one-step activation method of the precursor under CO_2 flow is rarely cited [8]. In this study, the novel production of activated carbon from various types of Malaysian agricultural wastes in presence of CO_2 flow was investigated. The kinetics of CO_2 adsorption into the activated carbon was also studied. Throughout the study, various kinetic models such as pseudo-first-order, pseudo-second-order, Elovich, and intra-particle model have been evaluated. In addition, the reliability of these kinetic models in predicting the adsorption capacity is accessed by linear regression coefficient ($0 < R^2 < 1$) and relative error (ε), which is defined as the following expression in Eq. (1).

$$\varepsilon(\%) = \left(q_{e,\mathrm{cal}} - q_{e,\mathrm{act}}\right) \Big/ q_{e,\mathrm{act}} \times 100\% \quad (1)$$

Based on Eq. (1), $q_{e,\mathrm{cal}}$ is referring to the measured value that is obtained from the kinetic analysis, whilst $q_{e,\mathrm{act}}$ is the actual or true value of the adsorption capacity, based on the experimental work.

* Corresponding author. Tel.: +60 5 3687642; fax: +60 5 3688205.
E-mail address: drsuzana_yusuf@petronas.com.my (S. Yusup).

0360-5442/$ – see front matter © 2013 Elsevier Ltd. All rights reserved.
http://dx.doi.org/10.1016/j.energy.2013.08.050

Table 1
Past and future trend of coal usage for electricity generation in Malaysia (based on Ref. [4]).

Year	Consumption ('000 tonnes)
2000	3634
2003	8408
2005	14,030
2006	14,492
2007	18,209
2008	19,095
2009[a]	21,000
2012[a]	28,000
2020[a]	36,000

[a] Projected.

Table 2
Chemical compositions of precursors (wt%).

Biomass	C	H	N	O[a]	S
Palm kernel shell	50.76	5.89	0.52	42.29	0.56
Palm mesocarp fibre	45.98	5.73	1.74	45.80	0.76
Rice husk	41.88	5.51	0.48	51.47	0.67
Coconut shell	50.08	6.02	0.05	43.25	0.62
Coconut fibre	45.86	5.72	0.42	47.40	0.61

[a] By differences.

2. Materials and methods

2.1. Raw material

Agricultural wastes that were used in this study for the production of activated carbon include CF (coconut fibre), CS (coconut shell), RH (rice husk), PMF (palm mesocarp fibre), and PKS (palm kernel shell) which were all acquired from a local market. The chemical composition of these materials was analyzed using a CHNS analyser (PE 2400 Series II CHNS/O), and is shown in Table 2. The agricultural wastes were dried in an oven (Carbolite) at 110 °C overnight to remove any moisture present, followed by grinding and sieving of the feedstock to the required particle size for experimentation. Then, the samples were preserved in an ultra-low relative humidity dry cabinet prior further use.

2.2. Adsorbent synthesis

The various agricultural wastes were synthesized to activated carbon in a vertical pyrolysis reactor. Factors that affect the activated carbon production include the properties of the starting material, the particle size, the heating rate, the gas flow rate, the temperature and the holding time. A complete investigation of the effects of these factors would require a large number of experiments. Thus, in this study, the Taguchi optimization approach was used to reduce total number of experimental runs by selecting an appropriate orthogonal array based on the required number of factors and levels [9]. Taguchi L_{25} was selected as the optimum experimental design tool in the study with six factors and five levels each, as shown in Table 3. Thus the activated carbons from the various agricultural wastes were synthesized according to the parameters in Table 4, which amounts to 25 experimental runs.

The Taguchi experimental data was analyzed using the S/N (Signal to Noise) ratio, to determine the significance of each factor on the adsorption capacity. The S/N ratio can be classified into three main categories – larger-is-better, smaller-is-better, and nominal-is-better characteristics, depending on the specific output and application to be optimized. Smaller-is-better is chosen for undesirable characteristics such as defect that is supposed to be ideally zero value, whilst the larger-is-better is utilized when the performances need to be maximized. Besides, the nominal-is-better is used for the process that needs to achieve specified values, and neither smaller nor higher value is desirable [10]. In this present work, as the adsorption capacity is intended to be higher in order to determine the effectiveness of the synthesized adsorbents, the S/N ratio of larger-is-better was used in this present work, and the formula used for S/N calculation is as shown in Eq. (2).

$$Y = -\log\left[\frac{1}{n}\left(n\sum_{i=1}^{n}\frac{1}{y_i^2}\right)\right] \quad (2)$$

Based on Eq. (2), n is the number of tests and y_i refers to the performance values in the ith experiment. Then, the mean of S/N ratio at each level for various parameters must be calculated. The difference between the highest and the lowest value of average S/N ratio (delta) measures the significance of the parameters towards the process.

2.3. CO_2 adsorption study

To determine the adsorption capacity of synthesized sorbent in capturing pure CO_2 (99.98% purity), a thermal gravimetric analyser (EXSTAR TG/DTA 6300) was used. A small amount of the agricultural wastes (5–10 mg samples) was used in the TGA (thermogravimetric analyser), with the temperature varied between 25 and 100 °C. After 2 h of adsorption process, CO_2 flow was switched to nitrogen (99.999% purity) to perform desorption process at the same temperature. In industrial application, CO_2 adsorption capacity at the stack temperature (temperature of combustion gases leaving the boiler) which is within the range of 100–120 °C is of interest [11]. Thus, to investigate the adsorption capacity of the synthesized activated carbon under similar conditions, the adsorption studies were carried out at 50 and 100 °C as well.

3. Results and discussion

3.1. Sorption capacity

Table 4 shows that the highest CO_2 uptake at room temperature is exhibited by CS sample at the operating conditions listed in experimental run 16, with adsorption capacity of approximately

Table 3
Design factors and levels.

Factors	Level 1	Level 2	Level 3	Level 4	Level 5
Precursors	Palm mesocarp fibre (PMF)	Palm shell (PKS)	Rice husk (RH)	Coconut shell (CS)	Coconut fibre (CF)
Particle size (μm)	250	355	500	710	1000
Heating rate (°C/min)	5	10	15	20	25
CO_2 flow rate (cm^3/min)	100	150	200	250	300
Temperature (°C)	500	600	700	800	900
Holding time (min)	15	30	45	60	90

Table 4
Preliminary CO_2 adsorption capacity at ambient temperature and pressure.

Run	Starting material	Particle size (μm)	Heating rate (°C/min)	CO_2 flow rate (cm^3/min)	Activation temperature (°C)	Holding time (min)	CO_2 uptake (mg/g)	S/N ratio[a]
1	PMF	250	5	100	500	15	11.27	21.04
2	PMF	355	10	150	600	30	19.81	25.94
3	PMF	500	15	200	700	45	32.67	30.28
4	PMF	710	20	250	800	60	51.67	34.26
5	PMF	1000	25	300	900	90	29.49	29.39
6	PKS	250	10	200	800	90	56.52	35.04
7	PKS	355	15	250	900	15	51.32	34.21
8	PKS	500	20	300	500	30	14.61	23.29
9	PKS	710	25	100	600	45	27.63	28.83
10	PKS	1000	5	150	700	60	45.17	33.10
11	RH	250	15	300	600	60	20.43	26.21
12	RH	355	20	100	700	90	33.57	30.52
13	RH	500	25	150	800	15	30.45	29.67
14	RH	710	5	200	900	30	45.36	33.13
15	RH	1000	10	250	500	45	16.30	24.24
16	CS	250	20	150	900	45	78.77	37.93
17	CS	355	25	200	500	60	30.33	29.64
18	CS	500	5	250	600	90	30.07	29.56
19	CS	710	10	300	700	15	46.73	33.39
20	CS	1000	15	100	800	30	54.26	34.69
21	CF	250	25	250	700	30	41.79	32.42
22	CF	355	5	300	800	45	45.79	33.22
23	CF	500	10	100	900	60	60.20	35.59
24	CF	710	15	150	500	90	12.91	22.32
25	CF	1000	20	200	600	15	14.67	23.33

[a] Based on larger-the-better characteristics.

79 mg CO_2/g. High carbon and low ash content is one of the factors for high CO_2 adsorption. According to the CHNS results of the activated carbon from various agricultural wastes (shown in Table 5), the activated carbon from CS in experimental run 16 (which had the highest CO_2 adsorption capacity) contains the highest carbon content, which is 88 wt%. High carbon percentage in the adsorbent may enhance the inter-particle force between the CO_2 molecules and activated carbon, and this binding force is named as London dispersion force. In addition, Boonpoke et al. [12] confirmed that the carbon and ash content of the activated carbon influenced the sorption capacity. Despite the comparable surface area and pore characteristics of both the rice husk- and bagasse-activated carbon in Boonpoke et al.'s work, high inorganic contents in rice husk-based activated carbon had lower CO_2 sorption capacity as compared to bagasse-based activated carbon. Boonpoke et al. [12] reported that the maximum adsorption capacity obtained at room temperature is 76.89 and 57.13 mg/g for bagasse and rice-husk activated carbon, respectively. Besides, CO_2 adsorption capacity of commercial activated carbon is found to be only 35 mg/g at the ambient conditions [13]. Thus, it proves that the preliminary CO_2 adsorption study at ambient temperature and pressure is higher than the published data.

Table 5
Chemical properties of synthesized activated carbons (wt%).

Run	CHNS analysis				
	C	H	N	S	O
1	58.74	3.21	1.91	0.45	35.70
2	66.23	2.91	1.59	0.40	28.88
3	68.92	2.10	1.23	0.33	27.42
4	72.10	1.60	1.01	0.27	25.02
5	65.60	1.63	0.75	0.22	31.81
6	87.06	1.99	0.61	0.34	10.02
7	86.79	1.52	0.83	0.30	10.57
8	70.18	3.78	0.70	0.43	24.92
9	74.63	3.11	0.82	0.38	21.07
10	83.02	2.66	0.94	0.35	13.04
11	54.21	2.59	0.61	0.36	42.24
12	53.96	1.93	0.71	0.31	43.10
13	53.98	1.70	0.60	0.28	43.45
14	56.09	0.98	0.58	0.22	42.15
15	50.24	2.98	0.60	0.45	45.75
16	88.18	1.32	0.40	0.25	9.87
17	75.47	3.60	0.25	0.49	20.21
18	80.52	3.21	0.24	0.44	15.60
19	83.95	2.74	0.24	0.38	12.70
20	86.92	1.93	0.41	0.30	10.45
21	65.70	2.33	0.62	0.30	31.05
22	68.89	1.90	0.47	0.28	28.47
23	66.90	1.67	0.45	0.25	30.75
24	62.03	3.18	0.73	0.42	33.66
25	64.43	3.21	0.62	0.42	31.33

Table 6 shows that the activation temperature has the most prominent effect on adsorptive properties of synthesized activated carbon in CO_2 capture, followed by precursors, holding time, gas flow rate, particle size, and heating rate. Temperature has a significant effect on the micro-porosity development of the activated carbon, which is very significant for gas phase adsorption, as the size of gas molecule varies from 0.4 to 0.9 nm [14]. Similar observations were made by Cao et al. [15], who reported that activation temperature was the most significant factor in the adsorption process, with improved adsorption efficiency at higher temperatures. However, Khare and Kumar [16] reported that temperature had the least effect on the adsorption process, whilst pH had the most significant effect. This discrepancy in the findings could be

Table 6
Response table for average S/N ratio of CO_2 sorption capacity (mg/g).

Level	1	2	3	4	5	Delta	Rank
Precursors	28.18	30.89	28.75	33.04	29.36	4.86	2
Particle size (μm)	30.53	30.70	29.68	30.37	28.95	1.75	5
Heating rate (°C/min)	30.01	30.84	29.52	29.87	29.99	1.32	6
Gas flow rate (cm^3/min)	30.13	29.77	30.29	30.94	29.10	1.84	4
Temperature (°C)	24.09	26.77	31.94	33.38	34.05	9.96	1
Holding time (min)	28.33	29.90	30.90	31.76	29.35	3.43	3

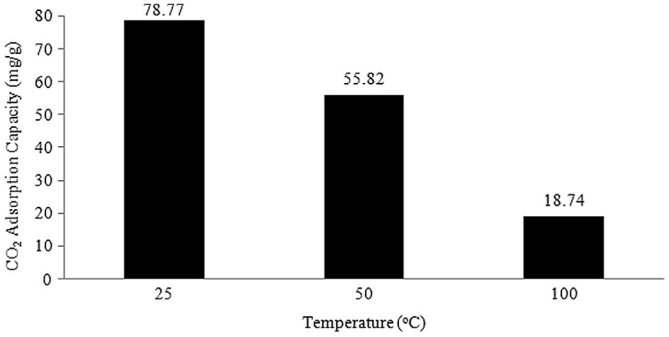

Fig. 1. CO_2 adsorption capacity of synthesized activated carbon at run 16 (material = coconut shell, particle size = 250 μm; heating rate = 20 °C/min; CO_2 flow rate = 150 cm^3/min; temperature = 900 °C; holding time = 45 min).

explained by the difference in characteristics and performance of the adsorbents, the nature of the precursors, the types of activating agent, as well as magnitude and range of the variables in the study [15].

Fig. 1 shows the CO_2 adsorption capacity of synthesized activated carbon from CS in experimental run 16 at temperatures of 50–100 °C. According to Fig. 1, it is revealed that CO_2 adsorption capacity decreased with increased in temperature. Le Chatelier principles outline that for an exothermic process i.e. physisorption, adsorption is favoured at lower temperatures. Thus, the high adsorption capacity at the lower temperatures in Fig. 1 implies the existence of physical adsorption behaviour throughout the process. This phenomenon is observed in other investigations in literature, which is presented in Table 7. Table 7 shows that the adsorption capacity of our study at both low and elevated temperature is greater compared to published data in literature [12,17–19]. Aside from the lower CO_2 adsorption capacity of the synthesized activated carbons from the chemical activation, other drawbacks of the chemical activation process include the waste disposal problems, and utilization of chemicals such as $ZnCl_2$ (zinc chloride) which are hazardous, corrosive and cost-intensive seems unattractive [20]. In contrast to CO_2-activation that develops the micropores and gradually widens them, steam-activation method on the other hand enlarges the micropores to mesopores from the beginning of the activation process [21], and thus results in lower adsorption capacity [18,19]. In this study, the synthesized activated carbons were physically activated with CO_2 as the activation agent, and thus will circumvent the drawbacks of chemical and steam activation as mentioned above.

Table 7
Comparisons study of CO_2 adsorption capacity onto carbonaceous adsorbents.

Material	Activation process	Adsorption capacity (mg/g)				Reference
		Room temperature[a]	323 K	348 K	373 K	
Coconut shell AC[b]	Physical (CO2)	78.77	55.82	–	18.74	This study
Bagasse AC	Chemical	76.89	–	24.30	–	[12]
Rice husk AC	(ZnCl2)	57.13	–	20.03	–	
Coconut shell char	Chemical (MEA)	45.58	–	–	–	[17]
Anthracites AC	Physical (steam)	58.00	40.00	28.00		[18]
Anthracites AC	Physical (steam)	60.90	–	21.68	–	[19]

[a] Room temperature is within range of 298–303 K.
[b] AC = activated carbon.

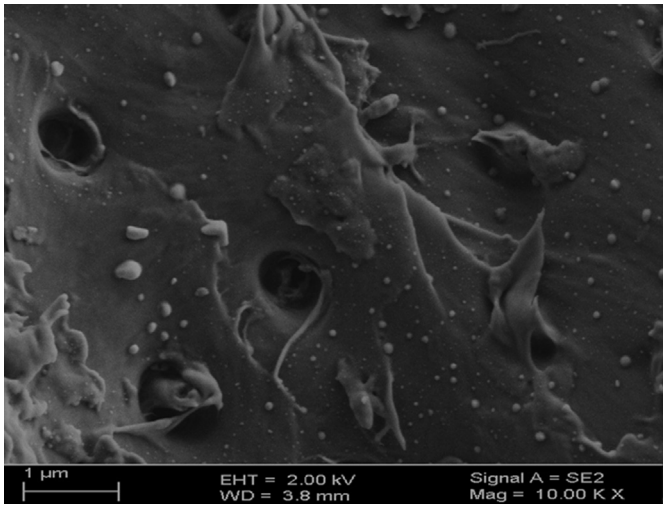

Fig. 2. FESEM image of the synthesized activated carbon at run 16 (material = coconut shell, particle size = 250 μm; heating rate = 20 °C/min; CO_2 flow rate = 150 cm^3/min; temperature = 900 °C; holding time = 45 min).

Apart from the carbon and ash content of the activated carbon, micro-porosity plays an important role on CO_2 adsorption capacity too [22]. Small micropores within the range of less than 0.7–1.0 nm are preferable because these sizes are responsible for the CO_2 uptake at 1 bar [22]. In addition, Boonpoke et al. [12] confirmed that the effective pore size for CO_2 adsorption at an ambient pressure is less than 1.0 nm, and yet the pore size of less than 0.26 nm is too narrow for CO_2 adsorption. For that reason, the median pore size of the optimized activated carbon (based on experimental run no. 16) was measured using the pore size analyzer, and it was found that the average pore size was approximately 0.574 nm. The findings in our study is in agreement with the published data by Wei et al. [22], who reported that the pore size of 0.55 nm was mainly responsible for CO_2 adsorption at low pressure, as it provides enough spaces for the molecules to accommodate themselves onto the pore wall. In this study, the existence of porosity on the synthesized activated carbon was examined using the Field Emission Scanning Electron Microscope as shown in Fig. 2. Based on Fig. 2, the smoother surface with some pore openings have been developed on the activated carbon. The development of the porosity on the exterior of the activated carbon structure is caused by the removal of inorganic

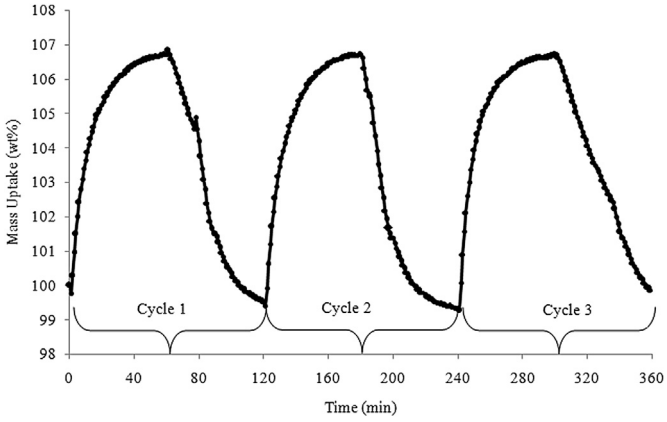

Fig. 3. Relationship of mass uptake of CO_2 against operation cycle[a] (material = coconut shell, particle size = 250 μm; heating rate = 20 °C/min; CO_2 flow rate = 150 cm^3/min; temperature = 900 °C; holding time = 45 min).

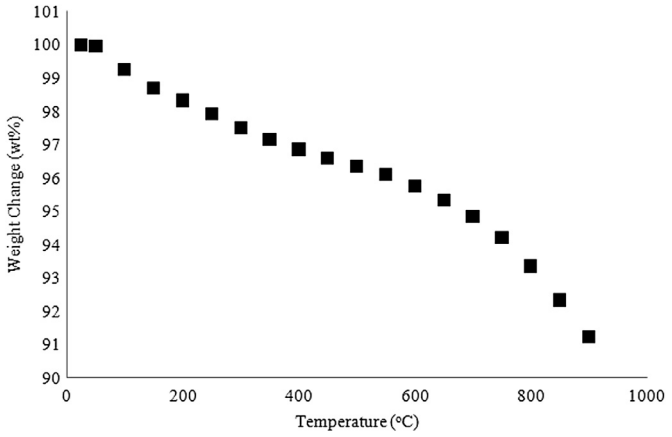

Fig. 4. TGA plot of synthesized activated carbon (material = coconut shell, particle size = 250 μm; heating rate = 20 °C/min; CO_2 flow rate = 150 cm^3/min; temperature = 900 °C; holding time = 45 min).

materials that tend to clog the pores. In addition, the development of porosity on the activated carbon after the physical activation indicates that there is a good opportunity for the CO_2 molecules to be trapped and adsorbed inside these pores.

Aside from the capacity of CO_2 adsorption, the reusability is another important characteristic of the adsorbents. Fig. 3 shows the adsorption cycle with respect to time for the activated carbon (run 16) at 25 °C. As can be seen, there is only a slight deviation of adsorption capacity over adsorption cycles, indicating the feasibility of this material to be utilized repeatedly. The repeatable of CO_2 adsorption in cyclic processes with lower variation in the CO_2 adsorption capacity suggests that the process is fully reversible, and complete regeneration can be obtained by evacuation of the CO_2 adsorbate during the desorption process.

The thermal stability is another measure of the degree of decomposition of activated carbon. It reflects the resistance towards heat and the mass loss during the activation process at elevated temperatures. Fig. 4 shows that the weight loss is minimal for the activated carbon used in this study, with only 10% weight loss at a temperature of 900 °C. Thus, the synthesized activated carbon is said to be less sensitive towards the temperature change over the range of temperature studied.

3.2. Kinetic analysis

The CO_2 adsorption onto the activated carbon at different operating temperature was modelled by using four kinetic models such as pseudo-first-order, pseudo-second-order, Elovich and intra-particle diffusion kinetic models.

3.2.1. Pseudo-first-order kinetic model

The earliest work that has been reported on kinetic study was conducted by Lagergren in 1898, as cited by Demirbas et al. [23]. The model which is often been used in liquid–solid phase is represented by Eq. (3) below.

$$dq_t/dt = k_1(q_e - q_t) \tag{3}$$

where q_t and q_e are the adsorption capacity at any particular time and at equilibrium respectively, and k_1 is the pseudo-first-order constant with unit of 1/min. Integrating Eq. (3) with the boundary equation results in a linearized form, as in Eq. (4). Hence, plotting graph of log $(q_e - q_t)$ versus time yields a linear function in which log (q_e) and $(k_1/2.303)$ is the y-intercept and slope, respectively.

$$\log\ (q_e - q_t) = \log\ (q_e) - (k_1/2.303)\cdot t \tag{4}$$

Table 8
Kinetic parameters of CO_2 adsorption onto activated carbon (material = coconut shell, particle size = 250 μm; heating rate = 20 °C/min; CO_2 flow rate = 150 cm^3/min; temperature = 900 °C; holding time = 45 min).

Kinetic model	Parameter	Temperature (°C)		
		25	50	100
	$(q_e)_{act}$ (mg/g)	78.772	55.818	18.740
Pseudo-first order model	k_1 (1/min)	0.039	0.032	0.018
	$(q_e)_{cal}$ (mg/g)	55.463	43.451	7.889
	R^2	0.983	0.985	0.887
	Relative error (%)	29.590	22.156	57.903
Pseudo-second order model	$(q_e)_{cal}$ (mg/g)	90.909	66.667	20.408
	k_2 (g/mg min)	9.680×10^{-4}	8.093×10^{-4}	3.892×10^{-3}
	h (mg/g min)	8.000	3.597	1.621
	R^2	0.999	0.999	0.996
	Relative error (%)	15.408	19.436	8.901
Elovich model	β (g/mg)	0.074	0.079	0.287
	α (mg/g min)	45.370	9.575	6.311
	R^2	0.978	0.984	0.927
Intra-particle diffusion model	k (mg/g $min^{1/2}$)	3.766	3.550	0.963
	C (mg/g)	40.860	19.430	8.526
	R^2	0.914	0.926	0.846

Kinetic parameters at each temperature and its corresponding coefficient of determination were summarized in Table 8. Based on Fig. 5, it was found that pseudo-first-order model does not fit well into the kinetic data, in addition to its low R^2 value as shown in Table 8, which is within the range of 0.89–0.98. Large deviation between experimental and calculated equilibrium capacity (q_e) was observed using this pseudo-first kinetic model.

3.2.2. Pseudo-second-order kinetic model

Apart from pseudo-first-order reaction model, pseudo-second-order reaction also is often cited in literature [23,24]. This type of reaction model that has been introduced by Ho et al. [24] is represented as follows:

$$t/q_t = 1/k_2\cdot q_e^2 + t/q_e \tag{5}$$

$$h = k_2\cdot q_e^2 \tag{6}$$

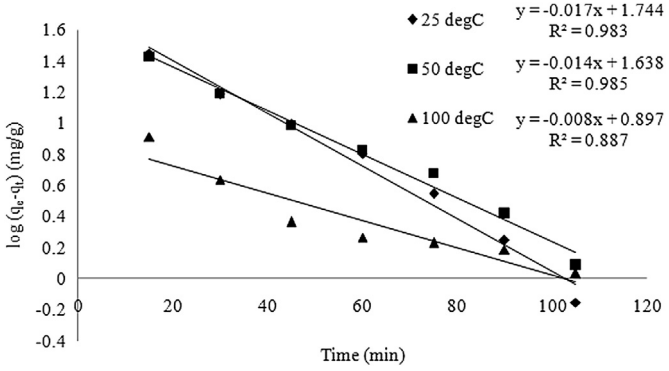

Fig. 5. Kinetic plot of pseudo-first-order model at various reaction temperatures (material = coconut shell, particle size = 250 μm; heating rate = 20 °C/min; CO_2 flow rate = 150 cm^3/min; temperature = 900 °C; holding time = 45 min).

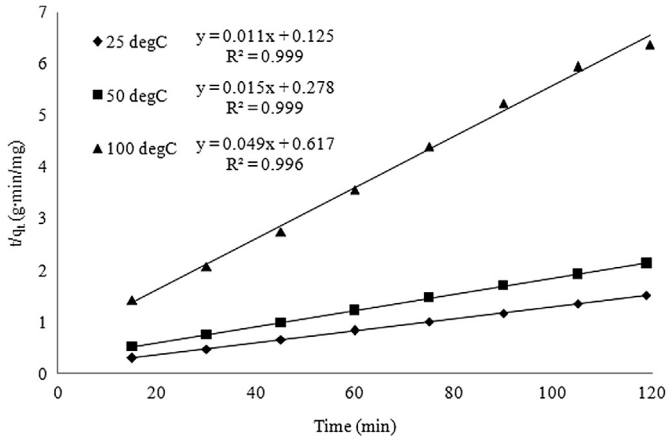

Fig. 6. Kinetic plot of pseudo-second-order model at various reaction temperatures (material = coconut shell, particle size = 250 μm; heating rate = 20 °C/min; CO_2 flow rate = 150 cm^3/min; temperature = 900 °C; holding time = 45 min).

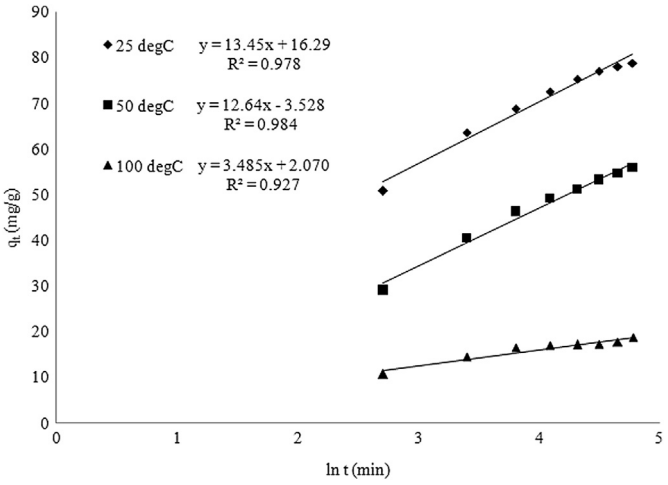

Fig. 7. Elovich plot of CO_2 adsorption onto synthesized activated carbon (material = coconut shell, particle size = 250 μm; heating rate = 20 °C/min; CO_2 flow rate = 150 cm^3/min; temperature = 900 °C; holding time = 45 min).

where k_2 is the pseudo-second-order rate constant, t is the contact time of gas–solid in min, while q_e and q_t is the adsorption capacity at equilibrium and particular time t, respectively, and h in Eq. (6) corresponds to the initial adsorption rate (mg/g min). Based on Fig. 6 and Table 8, it was evidently shown that pseudo-second-order-model fits the CO_2 adsorption profiles at various operating temperatures, with the regression coefficient values greater than 0.99. Besides, the relative error for the pseudo-second-order kinetic model is significantly lower compared to the pseudo-first-order model. Initial adsorption rate (h) that decreased with temperature verified the physisorption and exothermic behaviour of this process.

3.2.3. Elovich kinetic model

On the contrary of pseudo-first-order and second-order model, Elovich kinetic model is frequently applied in gas–solid reaction, and is expressed as follows [25]:

$$dq_t/dt = \alpha \exp(-\beta q_t) \tag{7}$$

where α is the initial adsorption rate (mg/g min), whilst β is the extent of surface coverage (g/mg) and activation energy of the process. The boundary conditions in which $\alpha\beta$ is assumed ≥ 1, $q_t = 0$ at $t = 0$ and $q_t = q_t$ at $t = t$ is being applied in Eq. (7), and upon integration, it results in new equation as shown in Eq. (8).

$$q_t = (1/\beta)\ln(\alpha\beta) + (1/\beta)\ln(t) \tag{8}$$

Based on Eq. (8), if the CO_2 adsorption fits the Elovich model, the Elovich plots of q_t versus ln (t) will yield a straight line with slope of $1/\beta$ and y-intercept of $1/\beta$ ln ($\alpha\beta$). Based on Table 8, the initial adsorption rate (α) decreased with temperature, similar to that of initial adsorption rate (h) in pseudo-second order model. The Elovich model describes the desorption process that is taking place as well, as the value of β is equivalent to the desorption rate [26]. As can be seen from Table 8, the magnitude of β which increased from 0.074 g/mg at 25 °C to 0.287 g/mg at 100 °C indicates that desorption was dominant. As shown in Fig. 7, Elovich kinetic model poorly fitted into the experimental data with the regression coefficient within 0.92–0.98.

3.2.4. Intra-particle diffusion kinetic model

In contrast with the above-mentioned kinetic models, intra-particle diffusion model provides the diffusion mechanism of the adsorption process. This model that is developed by Mckay et al. [27] is defined by Eq. (9).

$$q_t = kt^{1/2} + C \tag{9}$$

where q_t is the amount adsorbed at any particular time (mg/g), k is the intra-particle diffusion rate constant (mg/g $min^{1/2}$) and C (mg/g) relates to the thickness of boundary layer. If the adsorption process obeys the intra-particle diffusion model, a straight line plot of q_t against half power of time, $t^{1/2}$ passes through the origin is expected, with slope of k and y-intercept of C. In any of adsorption process, there are multiple steps that occurs such as mass transfer of adsorbate to adsorbent surface (bulk diffusion), film diffusion (external mass transfer resistance) and followed by surface diffusion into the internal sites (intra-particle diffusion) [26]. Fig. 8 shows the intra-particle diffusion plot for different reaction temperatures applied in this study and the corresponding kinetic parameters were tabulated in Table 8. As shown in Fig. 8, the deviation of the linear curve from the experimental data and does not passing through the origin suggests that the intra-particle diffusion is not the sole rate-limiting step in the adsorption process.

3.3. Evaluation of activation energy

Ease of adsorption process requires the minimum activation energy. Activation energy can be calculated by using the Arrhenius equation as shown in Eq. (10):

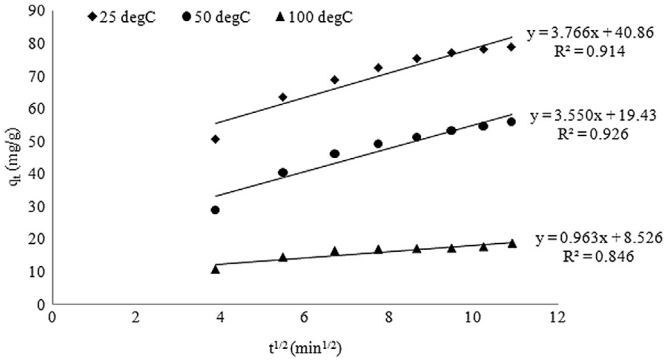

Fig. 8. Intra-particle diffusion model of CO_2 adsorption onto activated carbon (material = coconut shell, Particle size = 250 μm; heating rate = 20 °C/min; CO_2 flow rate = 150 cm^3/min; temperature = 900 °C; holding time = 45 min).

$$\ln k_2 = \ln k_0 - E_a/RT \quad (10)$$

According to Eq. (10), k_2 is pseudo-second-order constant (g/mg min), k_0 is the temperature independent factor (g/mg min), E_a is the apparent activation energy for adsorption (J/mol), R is the gas constant (8.314 J/mol K) and T is the adsorption temperature in K. Based on Eq. (10), plotting ln k_2 versus the reciprocal of temperature yields a straight line with y-intercept of ln k_0 and slope of $(-E_a/R)$. The activation energy of this present study was found to be approximately 17 kJ/mol. In physisorption process, the value of activation energy is typically low due to weak interaction forces between adsorbent and adsorbate, which is in contrast to chemisorption which takes place at elevated temperature and has high activation energy (42 kJ/mol) [28]. Thus, the lower value of the activation energy in this study shows that the CO_2 adsorption investigated in the current study falls under physisorption category.

4. Conclusion

In this study, several types of biomass have been investigated as the feedstock for the production of activated carbon for gas phase adsorption. The results show that high carbon content affects the CO_2 uptake onto the surface of activated carbon. The decrease of the adsorption capacity with increasing temperature and coupled with an ease of regeneration process indicates that mainly physisorption process is taking place during the adsorption process. In addition, the high correlation coefficient to unity implies the conformity of the pseudo-second order model with the experimental data. Besides, the value of activation energy proves that the adsorption process is a physical process.

Acknowledgements

The supports from Universiti Teknologi PETRONAS through Graduate Assistantship Scheme and NanoFund with Project number of NND/NA/(1)/TD11-036 provided by Ministry of Science, Technology and Innovation (MOSTI) are gratefully acknowledged.

References

[1] Safaai NSM, Noor ZZ, Hashim H, Ujang Z, Talib J. Projection of CO_2 emissions in Malaysia. Environ Prog Sustain Energy 2011;30:658–65.
[2] Othman MR, Martunus, Zakaria R, Fernando WJN. Strategic planning on carbon capture from coal fired plants in Malaysia and Indonesia: a review. Energy Policy 2009;37:1718–35.
[3] Oh TH, Pang SY, Chua SC. Energy policy and alternative energy in Malaysia: issues and challenges for sustainable growth. Renew Sustain Energy Rev 2010;14:1241–52.
[4] Oh TH. Carbon capture and storage potential in coal-fired plant in Malaysia—a review. Renew Sustain Energy Rev 2010;14:2697–709.
[5] Olajire AA. CO_2 capture and separation technologies for end-of-pipe applications – a review. Energy 2010;35:2610–28.
[6] Yang H, Xu Z, Fan M, Gupta R, Slimane RB, Bland AE, et al. Progress in carbon dioxide separation and capture: a review. J Environ Sci 2008;20:14–27.
[7] Kapdi SS, Vijay VK, Rajesh SK, Prasad R. Biogas scrubbing, compression and storage: perspective and prospectus in Indian context. Renew Energy 2005;30:1195–202.
[8] Yang K, Peng J, Xia H, Zhang L, Srinivasakannan C, Guo S. Textural characteristics of activated carbon by single step CO_2 activation from coconut shells. J Taiwan Inst Chem Eng 2010;41:367–72.
[9] Roy RK. Design of experiments using the Taguchi approach: 16 steps to product and process improvement. 1st ed. New York: Wiley; 2001.
[10] Kalpit J, Deepak K, Sanjay K. Plastic injection molding with Taguchi approach – a review. Int J Sci Res 2013;2:147–9.
[11] Nugteren H, Jones R, McCarthy M, Anderson M, Querol X, Moreno N, et al. Novel products and applications with combustion residues. In: Cox M, Nugteren H, Janssen-Jurkovičová M, editors. Combustion residues: current, novel and renewable applications. England: John Wiley & Sons; 2008. p. 199–378.
[12] Boonpoke A, Chiarakorn S, Laosiripojana N, Towprayoon S, Chidthaisong A. Synthesis of activated carbon and MCM-41 from bagasse and rice husk and their carbon dioxide adsorption capacity. J Sustain Energy Environ 2011;2:77–81.
[13] Thote JA, Iyer KS, Chatti R, Labhsetwar NK, Biniwale RB, Rayalu SS. In situ nitrogen enriched carbon for carbon dioxide capture. Carbon 2010;48:396–402.
[14] Guo J, Lua AC. Microporous activated carbons prepared from palm shell by thermal activation and their application to sulfur dioxide adsorption. J Colloid Interface Sci 2002;251:242–7.
[15] Cao Y, Pawłowski A, Zhang J. Preparation of activated carbons with enhanced adsorption of cationic and anionic dyes from Chinese hickory husk using the Taguchi method. Environ Prot Eng 2010;36:69–86.
[16] Khare P, Kumar A. Removal of phenol from aqueous solution using carbonized *Terminalia Chebula*-activated carbon: process parametric optimization using conventional method and Taguchi's experimental design, adsorption kinetic, equilibrium and thermodynamic study. Appl Water Sci 2012;2:317–26.
[17] Rebitanim NZ, Rebitanim NA, Ghani WAWAK, Yusup S, Mohd A, Mahmoud DK, et al. Carbon dioxide adsorption and desorption study on coconut shell biochar with nitrogen enrichment. J Dispersion Sci Technol 2013 [In press].
[18] Maroto-Valer MM, Tang Z, Zhang Y. CO_2 capture by activated and impregnated anthracites. Fuel Process Technol 2005;86:1487–502.
[19] Tang Z, Maroto Valer MM, Zhang Y. CO_2 capture using anthracite based sorbents. Prepr Pap – Am Chem Soc Div Fuel Chem 2004;49:298–9.
[20] Adinata D, Wan Daud WMA, Aroua MK. Preparation and characterization of activated carbon from palm shell by chemical activation with K_2CO_3. Bioresour Technol 2007;98:145–9.
[21] Rodríguez-Reinoso F, Molina-Sabio M, González MT. The use of steam and CO_2 as activating agents in the preparation of activated carbons. Carbon 1995;33:15–23.
[22] Wei H, Deng S, Hu B, Chen Z, Wang B, Huang J, et al. Granular bamboo-derived activated carbon for high CO_2 adsorption: the dominant role of narrow micropores. ChemSusChem 2012;5:2354–60.
[23] Demirbas E, Kobya M, Senturk E, Ozkana T. Adsorption kinetics for the removal of chromium (VI) from aqueous solutions on the activated carbons prepared from agricultural wastes. Water SA 2004;30:533–9.
[24] Ho YS, Mckay G, Wase D, Foster CF. Study of the sorption of divalent metal ions on to peat. Adsorpt Sci Technol 2000;18:639–50.
[25] Ekpete OA, Horsfall JM. Kinetic sorption study of phenol onto activated carbon derived from fluted pumpkin stem waste (*Telfairia occidentalis Hook. F*). J Eng Appl Sci 2011;6:43–9.
[26] Igwe JC, Abia AA. Adsorption kinetics and intra-particulate diffusivities for bioremediation of Co (II), Fe (II) and Cu (II) ions from waste water using modified and unmodified maize cob. Int J Phys Sci 2007;2:119–27.
[27] McKay G, Poots VJP. Kinetics and diffusion processes in colour removal from effluent using wood as an adsorbent. J Chem Technol Biotechnol 1980;30:279–92.
[28] Al-Ghouti M, Khraisheh MAM, Ahmad MNM, Allen S. Thermodynamic behaviour and the effect of temperature on the removal of dyes from aqueous solution using modified diatomite: a kinetic study. J Colloid Interface Sci 2005;287:6–13.